

See discussions, stats, and author profiles for this publication at: <https://www.researchgate.net/publication/260604077>

Prognostics of Chromaticity State for Phosphor-Converted White Light Emitting Diodes Using an Unscented Kalman Filter Approach

Article in IEEE Transactions on Device and Materials Reliability · March 2014

DOI: 10.1109/TDMR.2013.2283508

CITATIONS

19

READS

79

3 authors:



Jiajie Fan

Hohai University

65 PUBLICATIONS **377** CITATIONS

[SEE PROFILE](#)



Winco K.C. Yung

The Hong Kong Polytechnic University

172 PUBLICATIONS **2,859** CITATIONS

[SEE PROFILE](#)



Michael Pecht

University of Maryland, College Park

1,103 PUBLICATIONS **15,465** CITATIONS

[SEE PROFILE](#)

Some of the authors of this publication are also working on these related projects:



CALCE project at the university of maryland [View project](#)



Diagnostics and Prognostics of Electronic Circuits [View project](#)

Prognostics of Chromaticity State for Phosphor-Converted White Light Emitting Diodes Using an Unscented Kalman Filter Approach

Jiajie Fan, *Student Member, IEEE*, Kam-Chuen Yung, *Member, IEEE*, and Michael Pecht, *Fellow, IEEE*

Abstract—Phosphor-converted white light-emitting diodes (pc-white LEDs) utilize a blue LED chip converted by the phosphor to obtain white light emission. Pc-white LEDs have become one of the most popular white LEDs. The reliability concerns of pc-white LEDs involve both lumen maintenance and chromaticity state. However, previous research on the health of LEDs has not taken chromaticity state shift into consideration. Therefore, this paper investigates the chromaticity state shift of pc-white LEDs during an aging test using a data-driven prognostic approach. The chromaticity coordinates (u' , v') in the CIE 1976 color space are used to define the states of chromaticity. The Euclidean distance measures between two different chromaticity states represent the chromaticity state shift of LED after aging. A nonlinear dual-exponential model is selected to describe the chromaticity state shift process. Usually, the LED industry used an extrapolating approach to project future states of LED lighting sources, which relies on the nonlinear least square method to fit the obtained data and extrapolates the fitting curve to get the future state. In this paper, a recursive nonlinear filter (an unscented Kalman filter) is used to track the future chromaticity state. The result shows that the unscented Kalman filter approach can improve the prognostic accuracy more compared with the conventional extrapolating approach.

Index Terms—Phosphor-converted white LED, chromaticity state shift, prognostics, qualification testing, unscented Kalman filter (UKF).

I. INTRODUCTION

PHOSPHOR-CONVERTED white light emitting diodes (pc-white LEDs) have higher efficiency, smaller size, lower power, consumption, and higher reliability than traditional white light sources (such as incandescent lamp, cold cathode fluorescent lamp) [1]–[4]. Pc-white LEDs must undergo qualification testing before being released to market. However, most of the traditional qualification test techniques, such as Failure Modes, Mechanisms, and Effects Analysis (FMMEA), Fault Tree Analysis (FTA), the Lifetime Test, and

the Accelerated Life Test (ALT) [5], are time-consuming and expensive, especially for devices with long lifetimes. Sometimes the duration of the reliability test and assessment procedure is longer than time between product updates. Therefore, prognostic qualification testing based on historical test data is desirable for faster commercialization of pc-white LEDs.

From previous studies [6], [7], it has been found that both lumen depreciation and chromatic state shift are considered to be the two dominating failures in white LEDs. Most attention has been paid to the lumen depreciation of LED products [8]–[10], ignoring chromaticity state shift. In the LED industry, the Illuminating Engineering Society of North America (IESNA) (IES-LM-79-08 [11] and IES-LM-80-08 [12]) has recommended test methods for measuring the chromaticity characteristics of LEDs. Additionally, the Next Generation Lighting Industry Alliance (NGLIA), with the U.S. Department of Energy (DoE), has recommended using chromaticity shift as an indicator of a white LED's "end of life" [13]. The American National Standard Lighting (ANSI) group has also developed specifications for the chromaticity of solid state lighting products, but they have not demonstrated a chromaticity state shift prediction method for white LED lighting [14].

Prognostics and health management (PHM) is a technique used for fault diagnostics and reliability prediction in electronics-rich systems. There are three categories of approaches to PHM [15]–[17]: physics-of-failure (PoF), data-driven, and fusion. Among these three approaches, PoF-based PHM uses mathematical equations to predict the physics governing failures, which requires knowledge of the failure mechanisms, geometry of the system, material properties, and loading conditions. The data-driven approach relies on analysis of the *in situ* monitored data obtained from sensors to detect anomalies and predict the future state or remaining useful life of the system.

In this paper, we use chromatic coordinates (u' , v') in the CIE 1976 color space to represent the chromaticity state of the pc-white LED. The Euclidean distance is the difference between the original chromaticity coordinates (u'_0 , v'_0) and future coordinates (u'_i , v'_i); $\Delta u'v'$ is used to describe the chromaticity state shift after aging. Currently, there were several publications explained to the mechanisms of chromaticity state shift of pc-white LEDs [18], [19] (e.g., aging of LED chips, degradation of phosphor efficiency [20], discoloration of the encapsulations and lens [21], and so on). As so many root causes generating chromaticity state shift in pc-white LEDs, there is no specific physical model to describe this phenomenon. In this paper,

Manuscript received May 6, 2013; revised August 27, 2013; accepted September 20, 2013. Date of publication September 25, 2013; date of current version March 4, 2014. The work described in this paper was supported in part by the Research Committee of The Hong Kong Polytechnic University under a grant and in part by the Research Grants Council of the Hong Kong Special Administrative Region, China, under Grant CityU8/CRF/09.

J. Fan and K.-C. Yung are with the Printed Circuit Board Technology Centre, Department of Industrial and Systems Engineering, The Hong Kong Polytechnic University, Kowloon, Hong Kong (e-mail: jay.fan@connect.polyu.hk).

M. Pecht is with the Center for Advanced Life Cycle Engineering, University of Maryland, College Park, MD 20742 USA.

Color versions of one or more of the figures in this paper are available online at <http://ieeexplore.ieee.org>.

Digital Object Identifier 10.1109/TDMR.2013.2283508

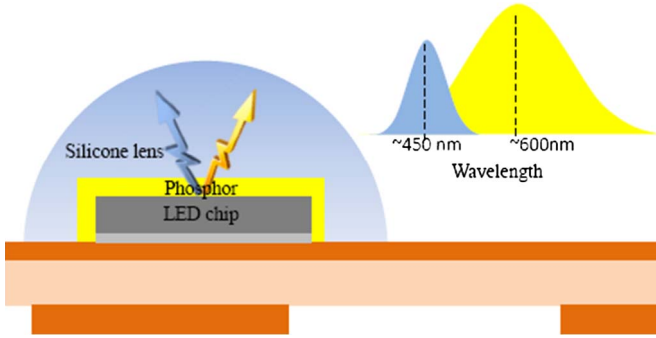


Fig. 1. White LUXEON Rebel and its luminescence mechanism.

we present a data-driven prognostic approach to predict the future chromaticity state based on the observed chromaticity state. First, we modeled the chromaticity state shift process by a nonlinear dual-exponential model. Then a recursive nonlinear filtering method (an Unscented Kalman Filter (UKF)) is utilized to predict the future chromaticity state. Finally, we compared the prognostic results to the extrapolated results.

The remainder of this paper is organized into four sections. Section II describes the research device and experimental procedure. Section III introduces the definition of chromaticity state and its shift and the implementation of the UKF approach. Section IV presents and discusses the results. Finally, the conclusions are presented in Section V.

II. RESEARCH DEVICE AND EXPERIMENTAL PROCEDURE

A. Research Device

The research device selected in this paper is a warm white LUXEON Rebel (Type LXM8-PW27), which is a type of high power pc-white LED with high luminous flux (> 100 lumens at 350 mA, Nominal Correlated Color Temperature (CCT) = 2700) produced by Philips [22]. Fig. 1 shows the packaging structure and luminescence mechanism of a white LUXEON Rebel. The mechanism for generating white light in a pc-white LED is a combination of blue light emitted by a GaN-based chip and excited yellow light emission from a YAG:Ce phosphor [20], [23], [24].

B. Experimental Procedure

Based on the approved test method recommended by IESNA (IES-LM-80-08), the experimental procedure included six cycles for 6000 hrs of operation. Each cycle involved three steps: aging, cooling, and testing (Fig. 2). For aging, the white LUXEON Rebel units were soldered onto a reliability test board that was thermally controlled by water cooling. The units were driven by a constant DC current in a thermal chamber. After 1000 hrs of aging, the reliability test board was removed from the thermal chamber to be cooled to room temperature. For testing, the lumen flux, forward voltage, and chromaticity coordinates of each sample were measured underneath the integrating sphere. After testing, the reliability stress board was returned to the thermal chamber to undergo the next aging cycle.

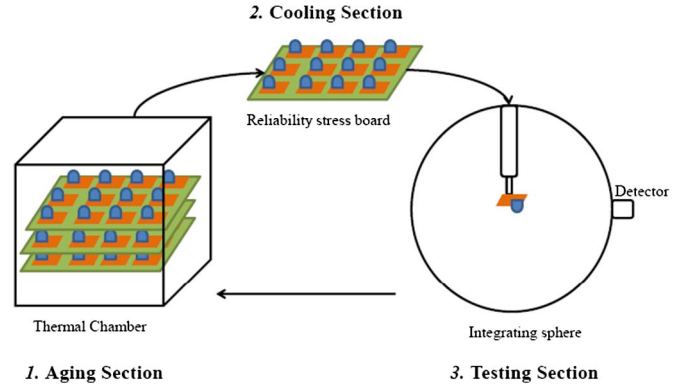


Fig. 2. Experimental procedure.

TABLE I
IES LM-80-08 AGING AND TESTING CONDITIONS

| Items | |
|---------------------|----------|
| Aging Temperature | 55 °C |
| Testing Temperature | 25 ±2°C |
| Input Current | 350 mA |
| Relative Humidity | <65% |
| Sample size | 25 |
| Test duration | 6,000hrs |

This paper selected the lowest stress aging conditions from the LM-80 test report [DR04: LM-80 Test Report, LUMILEDS, PHILIPS] [25], which was the condition most similar to normal operation. The condition parameters are listed in Table I.

III. CHROMATICITY STATE AND PROGNOSTICS METHODOLOGY

A. Chromaticity State Shift of pc-White LED

According to the approved electrical and photometric measurement method developed by IESNA [10], [11], the chromaticity characteristics of white LEDs include the chromaticity coordinates, correlated color temperature, and color rendering index (CRI). Among them, chromaticity coordinates were always chosen as the direct performance parameters to track the shift path.

The International Commission for Illumination (*Commission Internationale de l'Eclairage*, CIE) has developed three types of chromaticity diagrams [27]: CIE 1931 (x, y), CIE 1960 uniform chromaticity scale (UCS) (u, v), and CIE 1976 UCS (u', v') (Fig. 3). Among them, only the color difference in the CIE 1976 color space is proportional to the geometric difference, so the chromaticity coordinates in the CIE 1976 color space are widely used as a chromaticity performance characteristic by many LED manufacturers. The (u', v') uniform chromaticity coordinates can be calculated as follows:

$$u' = \frac{4x}{-2x + 12y + 3} \quad (1)$$

$$v' = \frac{9y}{-2x + 12y + 3} \quad (2)$$

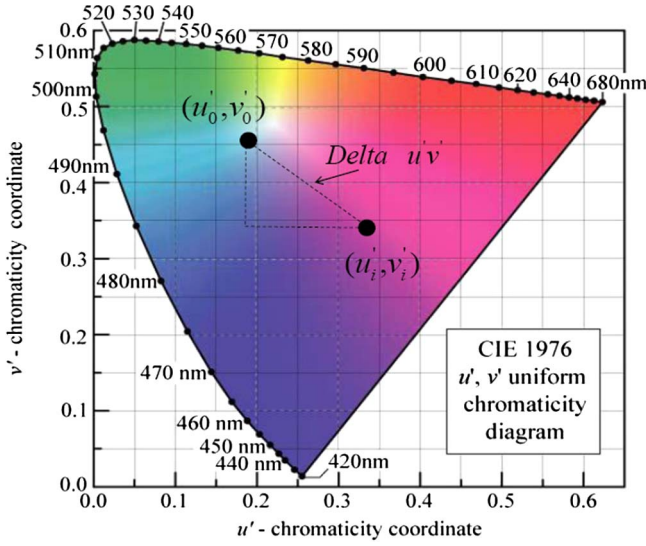


Fig. 3. CIE 1976 (u' , v') uniform chromaticity diagram [2].

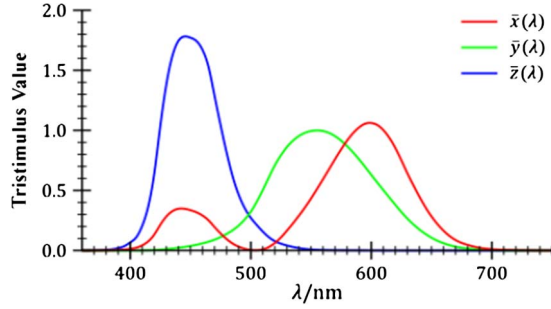


Fig. 4. Color matching function [26].

$$x = \frac{X}{X + Y + Z} \quad (3)$$

$$y = \frac{Y}{X + Y + Z} \quad (4)$$

$$X = \int_{\lambda} \bar{x}(\lambda) P(\lambda) d\lambda \quad (5)$$

$$Y = \int_{\lambda} \bar{y}(\lambda) P(\lambda) d\lambda \quad (6)$$

$$Z = \int_{\lambda} \bar{z}(\lambda) P(\lambda) d\lambda \quad (7)$$

where X , Y , and Z are defined as tristimulus values to simulate the primary red, green, and blue lights, respectively, needed to match the color of a given power-spectral density $P(\lambda)$. The matching functions $\bar{x}(\lambda)$, $\bar{y}(\lambda)$, and $\bar{z}(\lambda)$ are shown in Fig. 4.

In this paper, the collected chromaticity coordinates in the CIE 1976 color space from the LM-80 test report were selected to represent the chromaticity state of the white LUXEON Rebel LED [22]. The Euclidean distance between the original chromaticity coordinates (u'_0, v'_0) and future coordinates (u'_i, v'_i)

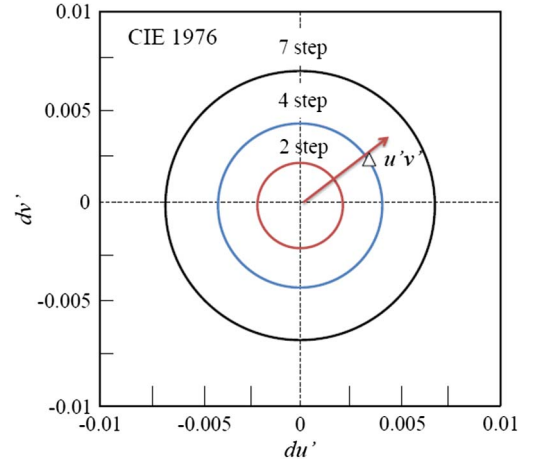


Fig. 5. Approximate n-step SDCM in CIE 1976 chromaticity diagram [28].

was used to represent the chromaticity state shift of the LED after aging which is denoted by $\Delta u'v'$ (Fig. 3)

$$\Delta u'v' = \sqrt{(du')^2 + (dv')^2} = \sqrt{(u'_i - u'_0)^2 + (v'_i - v'_0)^2}. \quad (8)$$

The International Electrotechnical Commission (IEC) has developed an approach to characterizing chromaticity and chromaticity shift based on specific chromaticity coordinates, which can be defined in terms of numbers of “standard deviations of color matching (SDCM)” (see Fig. 5). A LED product should be considered as failed for excessive chromaticity state shift if it moves outside a boundary. The boundary is defined as terms of n-step SDCM (or n-step MacAdam ellipse) [28].

Based on the different applications of LED products, the criteria of chromaticity state shift failure can be categorized as follows:

- 2-step SDCM: for applications where the white LED lightings are placed side-by-side and are directly visible, or when these lightings are used to illuminate an achromatic (white) scene. For example, accent lighting a white wall and lighting a white cove.
- 4-step SDCM: for applications where the white LED lightings are not directly visible, or when these lightings are used to illuminate a visually complex, multicolored scene. For example, lighting a display case and accent lighting multicolored objects or paintings.
- 7-step SDCM: this criteria is accepted by both ANSI and ENERGY STAR Program of DoE to qualify general lighting [29].

B. Unscented Kalman Filter

The Unscented Kalman Filter (UKF) was first developed by Julier *et al.* [30]–[32] to estimate the state of nonlinear systems by using a deterministic sampling approach (sigma point sampling) to capture mean and covariance estimates with a minimal set of sample points. Compared to the other nonlinear state estimation methods, such as Extended Kalman Filter (EKF) and Particle Filter (PF), UKF has the following advantages: first, UKF eliminates the calculation of Jacobian and Hessian matrices in EKF and makes the estimation procedure easier; second, it increases the estimation accuracy by considering at

least the second order Taylor expansion (EKF just uses the first order Taylor approximation); third, it develops an optimal sampling approach (sigma point sampling), whereas the Monte Carlo random sampling approach used in PF does not [33].

UKF involves estimation of the state of a discrete-time nonlinear dynamic system, which can be represented by both a state model and a measurement model

$$\text{State model} \quad x_k = f_k(x_{k-1}, v_{k-1}) \quad (9)$$

$$\text{Measurement model} \quad y_k = h_k(x_k, n_k) \quad (10)$$

where x_k represents the unobserved state of the system, y_k is the observed measurements, v_{k-1} and n_k are the state noise and observation noise, respectively, and $v_{k-1} \sim N(0, Q_{k-1})$ and $n_k \sim N(0, R_k)$ are assumed to be mean zero white Gaussian noises.

The algorithm implementation of UKF can be expressed as follows:

Step I: Initialization

The initial state is described by its mean and covariance

$$\bar{x}_0 = E[x_0] \quad (11)$$

$$P_0 = E[(x_0 - \bar{x}_0) \cdot (x_0 - \bar{x}_0)^T]. \quad (12)$$

Supposing that both noises are non-additive, the initial state vector and covariance matrix can be expressed as an augment vector

$$\bar{x}_0^a = E[x_0^a] = [\bar{x}_0^T \quad 0 \quad 0]^T \quad (13)$$

$$P_0^a = \begin{bmatrix} P_0 & 0 & 0 \\ 0 & Q_0 & 0 \\ 0 & 0 & R_0 \end{bmatrix}. \quad (14)$$

Step II: Sigma point sampling

To undergo an unscented transform (UT), we develop a matrix χ_k^a with $2n_a + 1$ sigma points based on the mean and covariance to preserve the nonlinear nature of the system. Until now, there are several variations of UT developed by others [34], like basic UT, general UT, simplex UT and Spherical UT. This paper chose the general UT to conduct sigma point sampling, because it generates a symmetric optimal sigma-point matrix to represent nonlinear system

$$\chi_k^a = \begin{bmatrix} \bar{x}_{k-1}^a & \bar{x}_{k-1}^a + \sqrt{n_a + \lambda} \\ & \cdot \sqrt{p_{k-1}^a} & \bar{x}_{k-1}^a - \sqrt{n_a + \lambda} \cdot \sqrt{p_{k-1}^a} \end{bmatrix} \quad (15)$$

$$n_a = n_x + n_v + n_n \quad (16)$$

$$\lambda = \alpha^2(n_a + k) - n_a. \quad (17)$$

Then the sigma points are weighted by

$$W_0^{(m)} = \frac{\lambda}{n_a + \lambda} \quad (18)$$

$$W_0^{(c)} = \frac{\lambda}{n_a + \lambda} + (1 - \alpha^2 + \beta) \quad (19)$$

$$W_i^{(m)} = W_i^{(c)} = \frac{1}{2(n_a + \lambda)} \quad i = 1, 2, \dots, 2n_a \quad (20)$$

where λ is the composite scaling parameter, which can be calculated from equation (17). The constant α determines the spread of sigma points around the mean ($1 \geq \alpha \geq 10^{-4}$); κ is a secondary scaling parameter which is usually set to $3 - n_a$, and β is used to incorporate prior knowledge of the distribution of the state vector x (for Gaussian distribution, $\beta = 2$). In this paper, we set $\alpha = 0.01$, $\kappa = 3 - n_a$, and $\beta = 0$.

Step III: Time update

Estimate the transient state $\bar{x}_{k/k-1}$ and measurement $\bar{y}_{k/k-1}$

$$\chi_{k/k-1}^x = f(\chi_{k-1}^x, \chi_{k-1}^v) \quad (21)$$

$$\bar{x}_{k/k-1} = \sum_{i=0}^{2n_a} W_i^{(m)} \chi_{i,k/k-1}^x \quad (22)$$

$$P_{k/k-1} = \sum_{i=0}^{2n_a} W_i^{(c)} \left[\left(\chi_{i,k/k-1}^x - \bar{x}_{k/k-1} \right) \cdot \left(\chi_{i,k/k-1}^x - \bar{x}_{k/k-1} \right)^T \right] \quad (23)$$

$$y_{k/k-1} = h(\chi_{k-1}^x, \chi_{k-1}^n) \quad (24)$$

$$\bar{y}_{k/k-1} = \sum_{i=0}^{2n_a} W_i^{(m)} y_{i,k/k-1}. \quad (25)$$

Step IV: Measurement update

Calculate the cross-covariance of the state and measurement $P_{k/k-1}^{xy}$ and the Kalman gain K_k . Compute the predicted mean \bar{x}_k and covariance P_k

$$P_{k/k-1}^{yy} = \sum_{i=0}^{2n_a} W_i^{(c)} \left[\left(y_{i,k/k-1} - \bar{y}_{k/k-1} \right) \cdot \left(y_{i,k/k-1} - \bar{y}_{k/k-1} \right)^T \right] \quad (26)$$

$$P_{k/k-1}^{xy} = \sum_{i=0}^{2n_a} W_i^{(c)} \left[\left(\chi_{i,k/k-1}^x - \bar{x}_{k/k-1} \right) \cdot \left(y_{i,k/k-1} - \bar{y}_{k/k-1} \right)^T \right] \quad (27)$$

$$K_k = P_{k/k-1}^{xy} \left(P_{k/k-1}^{yy} \right)^{-1} \quad (28)$$

$$\bar{x}_k = \bar{x}_{k/k-1} + K_k(y_k - \bar{y}_{k/k-1}) \quad (29)$$

$$P_k = P_{k/k-1} - K_k P_{k/k-1}^{yy} K_k^T. \quad (30)$$

Fig. 6 shows the implementation procedure for prognostics with the UKF approach, which involves two major steps: filtering and prognostics. First, filtering is conducted recursively with both time and measurement updates. Then, when the measurement is terminated, the future $k + 1 \dots n$ step states are predicted with the k -step measures and the time updates from $k + 1$ to the desired step.

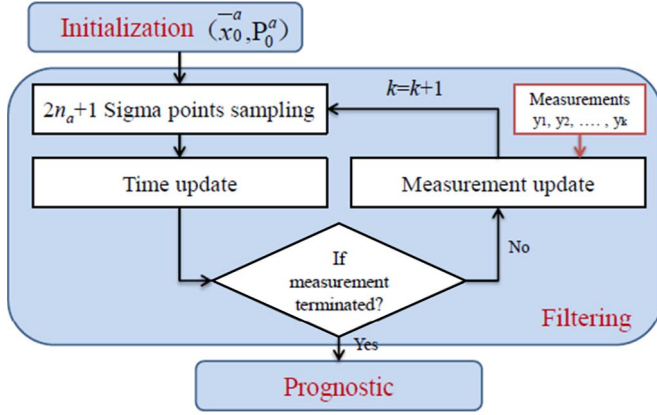


Fig. 6. Flowchart of UKF prognostics approach.

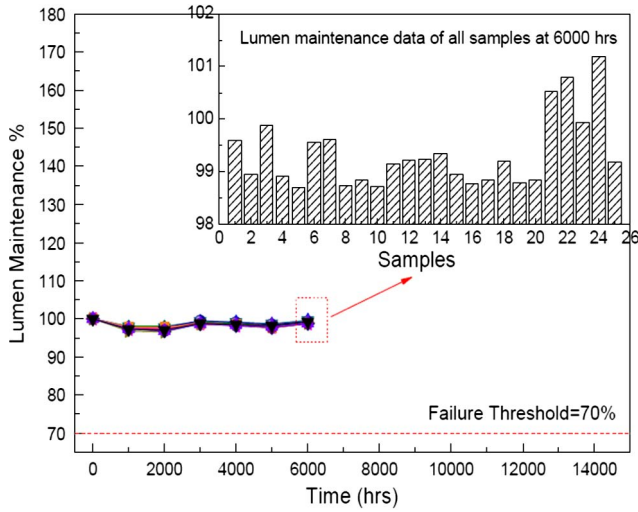


Fig. 7. Lumen maintenance data of all samples.

IV. RESULTS AND DISCUSSION

A. Test Result Analysis From LM-80 Report

According to the experimental procedure shown in Section II, the lumen flux, forward voltage, and chromaticity coordinates of each sample were collected every 1000 hrs. And the total data collected after 6000 hrs were documented as a LM-80 test report. The LM-80 report has been widely accepted by many LED manufacturers as a product specification to introduce their product's performances to customers. In this report, the degradation of LED product's performance can be indicated by three parameters collected over time (e.g., lumen flux, forward voltage, and chromaticity coordinates).

Lumen maintenance is the luminous flux remaining output (typically expressed as a percentage of the maximum output) at any selected elapsed operating time, which is also the converse of lumen depreciation. The Alliance for Solid-State Illumination Systems and Technologies (ASSIST) recommends the lumen failure threshold for general lighting as the 70% light output maintained over time (L70) [35]. As shown in Fig. 6, the lumen maintenance of all samples decreased in the initial 2000 hrs and then maintained above 95% stably. This means that all of LED samples did not fail in the light output performance during this 6000 hrs aging test.

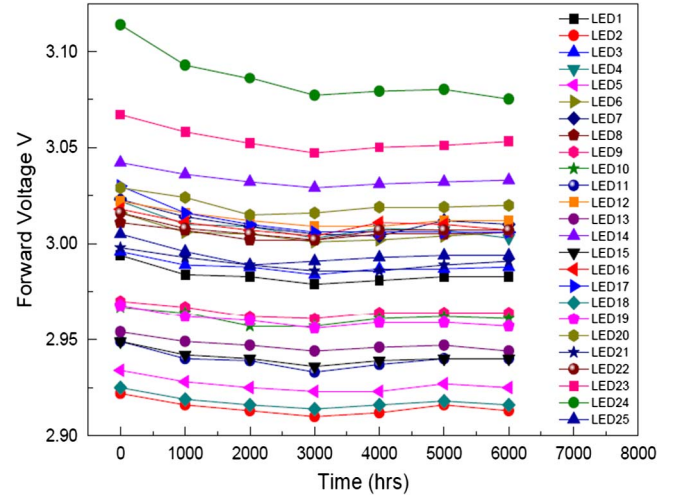
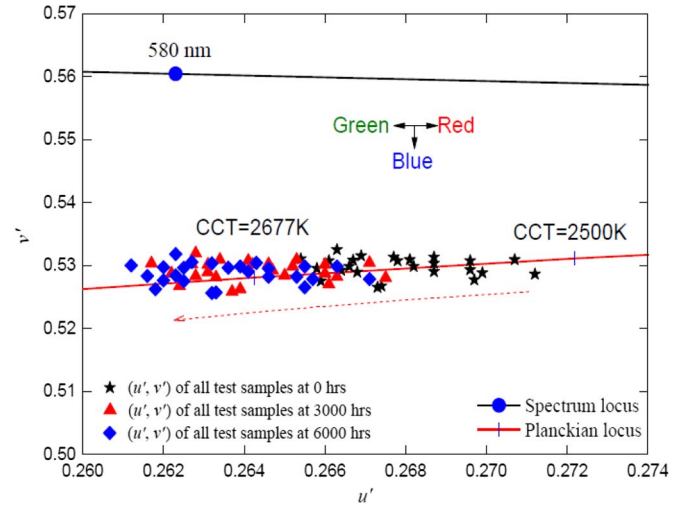


Fig. 8. Forward voltages of all samples.

Fig. 9. Chromaticity coordinates (u' , v') of all samples at 0, 3000 and 6000 hrs.

Forward voltage is another indicator to represent the performance of LED chip, which is a required energy to inject electron and drive the electron-hole recombination [2]. From the figure of the forward voltage over time (Fig. 8), it shows that the forward voltage of all samples dropped slightly before 3000 hrs and then kept relatively stable after 3000 hrs.

As introduced in Section III, the chromaticity coordinates (u' , v') in the CIE 1976 color space were selected to represent the chromaticity state of LEDs. Fig. 9 shows the chromaticity coordinates shift process of all samples after 6000 hrs aging. This shift process in first 3000 hrs was faster than that after 3000 hrs, which may be attributed to the degradation of forward voltage as shown in Fig. 8. With the increasing of aging time, the chromaticity coordinates shifted along with the Planckian locus and the CCT values increased about 100 K during 6000 hrs. This indicates that the colors of all LEDs were still white after aging but this white became cooler than the initial one.

Based on the equation (8), the Euclidean distance between the original chromaticity coordinates (u'_0, v'_0) and the

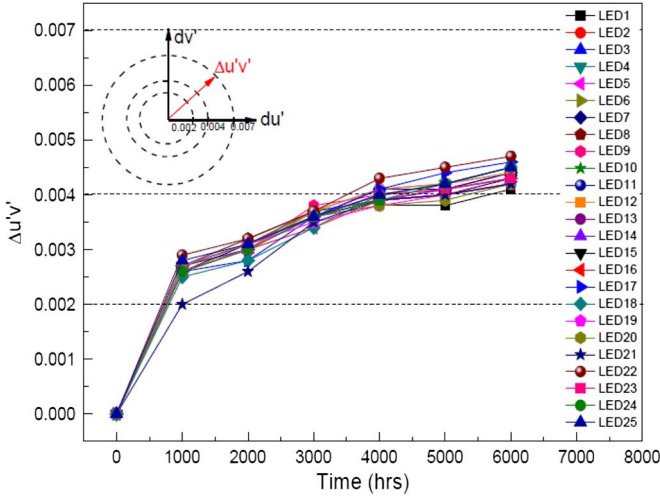


Fig. 10. Chromaticity state shift of all samples.

coordinates (u'_i, v'_i) collected after aging was used to represent the chromaticity state shift of the LEDs. The chromaticity coordinate shift of all samples during 6000 hrs aging (Fig. 9) can be transformed as the Euclidean distance shift (Fig. 10). According to the defined failure criteria in Section III, these test results can be accepted within the 7-step SDCM criteria, but will be defined as chromaticity failure by both 2-step and 4-step SDCM thresholds.

By summarizing of the test results in the LM-80 report, the degradation of light output performances of all samples were relatively acceptable after 6000 hrs aging (lumen maintenance $> 95\%$), however, their chromaticity performances degrades fast in this test. Therefore, prognostics of chromaticity state shift have become a meaningful topic in this LED qualification testing.

B. Prognostics of Chromaticity State Shift With UKF Approach

Because there is no specific physical model to describe chromaticity state shift, we present a data-driven prognostic approach (recursive UKF) in this paper to predict the future chromaticity state based on the observed chromaticity state. The theory of UKF was introduced in Section III, we developed a procedure in this section to evaluate this proposed approach, which includes four steps: (1) Calibration test (Model selection and Training model); (2) Filtering and prognostics; (3) Sensitivity analysis (Fig. 11).

1) Calibration Test:

a) *Model selection:* To begin with, this paper developed a model for the chromaticity state shift of our research device. We chose three models (exponential, dual-exponential, and quadratic polynomial) to fit the chromaticity state shift data, $\Delta u'v'$, with the nonlinear least square techniques in the Matlab curve fitting toolbox. Ten samples were selected from a total of twenty-five samples to train the selected model and initialize the parameters of the model. The remaining fifteen samples were used to test the proposed prognostics model.

The averaged chromaticity state shift data of ten training samples at each test cycle were fitted by three proposed models.

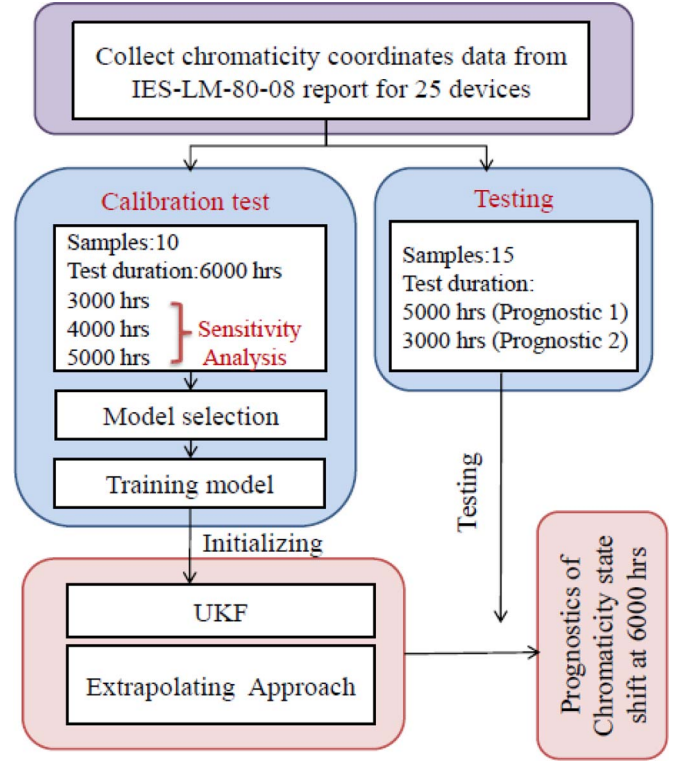


Fig. 11. Implementation flowchart of methodology.

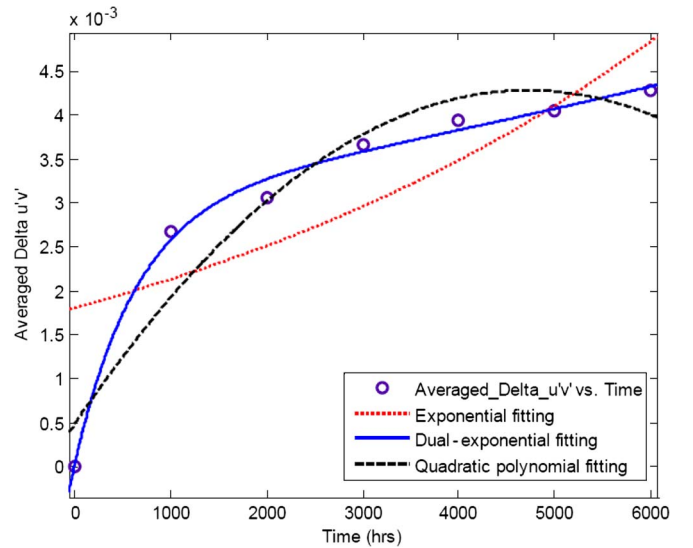


Fig. 12. Model selection for the chromaticity state shift process.

TABLE II
CHROMATICITY SHIFT PROCESS MODEL SELECTION RESULTS

| Models | | Averaged R-square | Averaged RMSE |
|----------------------|---|-------------------|---------------|
| Exponential | $y = a \cdot \exp(b \cdot x)$ | 0.62403 | 0.0009927 |
| Dual-exponential | $y = a \cdot \exp(b \cdot x) + c \cdot \exp(d \cdot x)$ | 0.99337 | 0.0001681 |
| Quadratic Polynomial | $y = a \cdot x^2 + b \cdot x + c$ | 0.92191 | 0.000505 |

The fitting results are shown in Fig. 12 and Table II. The results indicate that the dual-exponential model was the best model to describe the process of chromaticity state shift because its

TABLE III
PARAMETERS OF MEASUREMENT MODEL OBTAINED FROM
TRAINING SAMPLES

| No. | a | b | c | d |
|----------|-------------|-------------|-----------|-----------|
| 1 | 0.003014 | 5.13E-05 | -0.00301 | -0.001766 |
| 2 | 0.00311 | 5.28E-05 | -0.003078 | -0.001414 |
| 3 | 0.002852 | 7.42E-05 | -0.002844 | -0.001649 |
| 4 | 0.002726 | 8.58E-05 | -0.002722 | -0.002156 |
| 5 | 0.00275 | 8.00E-05 | -0.002746 | -0.00214 |
| 6 | 0.002837 | 7.33E-05 | -0.002833 | -0.001931 |
| 7 | 0.00289 | 7.32E-05 | -0.002883 | -0.001773 |
| 8 | 0.00313 | 5.21E-05 | -0.003099 | -0.001427 |
| 9 | 0.00306 | 6.09E-05 | -0.003034 | -0.001331 |
| 10 | 0.00311 | 5.28E-05 | -0.003078 | -0.001414 |
| Mean | 0.0029479 | 0.000065625 | -0.002933 | -0.0017 |
| STD | 0.000154884 | 1.31008E-05 | 0.0001436 | 0.0003058 |
| Variance | 2.3989E-08 | 1.71632E-10 | 2.063E-08 | 9.35E-08 |

averaged R-square is nearest to 1 and it also has the smallest averaged RMSE.

b) *Training model*: The state and measurement models in the UKF approach can be written as follows:

State model:

$$\begin{aligned}
 x_k &= [a_k; b_k; c_k; d_k] \\
 a_k &= a_{k-1} + \nu_{k-1}^a \quad \nu_{k-1}^a \sim N(0, Q_v^a) \\
 b_k &= b_{k-1} + \nu_{k-1}^b \quad \nu_{k-1}^b \sim N(0, Q_v^b) \\
 c_k &= c_{k-1} + \nu_{k-1}^c \quad \nu_{k-1}^c \sim N(0, Q_v^c) \\
 d_k &= d_{k-1} + \nu_{k-1}^d \quad \nu_{k-1}^d \sim N(0, Q_v^d). \quad (31)
 \end{aligned}$$

Measurement model:

$$\begin{aligned}
 y_k &= a_k \cdot \exp(b_k \cdot 1000 \cdot k) + c_k \cdot \exp(d_k \cdot 1000 \cdot k) \\
 &\quad + n_k n_k \sim N(0, R_k) \quad (32)
 \end{aligned}$$

where $k = 1, 2 \dots 7$ (from 0 to 6000 hrs).

The parameters of the dual-exponential model of each training sample were estimated by the nonlinear least square method and averaged as the initial states of the test samples ($a_0 = 0.0029479$; $b_0 = 0.000065625$; $c_0 = -0.002933$; $d_0 = -0.0017$) (Table III).

2) *Filtering and Prognostics*: Next, the test data from two filtering periods (Period I: 0–5000 hrs and Period II: 0–3000 hrs) were selected to update the states recursively, and then the chromaticity state shift at 6000 hrs was predicted based on these two filtering periods. The prognostic results of fifteen test samples are shown in Fig. 13, which indicates that the predicted result based on the period I data (UKF Prognostic 1) was slightly better than the results from the period II data (UKF Prognostic 2), because it utilized more observed measurements to update the state model (Fig. 14). The prognostic RMSE from

the two periods of data were 3.70% and 3.90%, respectively, and both predicted results were closed to the real state

$$RMSE = \sqrt{\frac{1}{15} \sum_{i=1}^{15} (\bar{y}_i - y_i)^2} \quad (33)$$

where y_i is the i th real $\Delta v'$ and \bar{y}_i bar is the predicted $\Delta v'$ at 6000 hrs.

This paper also compared the prognostic performances between the UKF approach and an extrapolating approach. The extrapolating approach is widely used to project long term lumen maintenance of LED lighting sources [36]. It relies on the nonlinear least square method to fit the obtained data and extrapolates the fitting curve to get the future state. Although both are the nonlinear estimation approaches, there are some differences between least square method and UKF approach: First, the UKF deals with dynamic stochastic systems while the least square is used for deterministic systems; Secondly, the UKF updates system states recursively with absorbing new measurements while the least square implementation uses batch processing [37]. In this paper, the two periods of data as mentioned were also extrapolated to get the chromaticity state of samples at 6000 hrs which were denoted as the Extrapolating 1 (for Period I) and the Extrapolating 2 (for Period II), respectively. The prediction results are listed in Table IV, which shows that compared to the extrapolating approach, the UKF approaches with lower prognostics errors (less than 4%) increased the prognostic accuracy more, even within a shorter data-collection time period. The reason is that UKF utilized the whole information from the collected data at each test cycles and updated the state model from new measurement inputs step by step, and it also had the ability to model the dynamic stochastic states of chromaticity shift which were driven by the random process noise, while the extrapolating approach estimated the parameters of the measurement model with the batch measurement data to predict the future state. Therefore, with the proposed UKF based prognostic approach, the data collection time in the reliability test for LEDs can be shortened from the standard minimum required 6000 hrs to 5000 hrs, or even 3000 hrs.

3) *Sensitivity Analysis*: In this section, we study the sensitivity of the prognostic performance of the proposed UKF approach (which can be evaluated by prognostic errors) by changing in the values of the initial states which were estimated from different calibration tests. Following the process of model-training, the initial states of test samples were estimated from curve-fittings for ten training samples. Here, we selected four types of calibration test with different time periods (3000 hrs, 4000 hrs, 5000 hrs and 6000 hrs) and fitted each time period data with the dual-exponential model. The parameters of the dual-exponential model of each training sample were estimated by the nonlinear least square method and averaged as the initial states of the test samples (Table V).

The UKF prognostic results were shown in Fig. 15, which indicates the values of initial states estimated from different calibration tests can influence the final prognostic performance

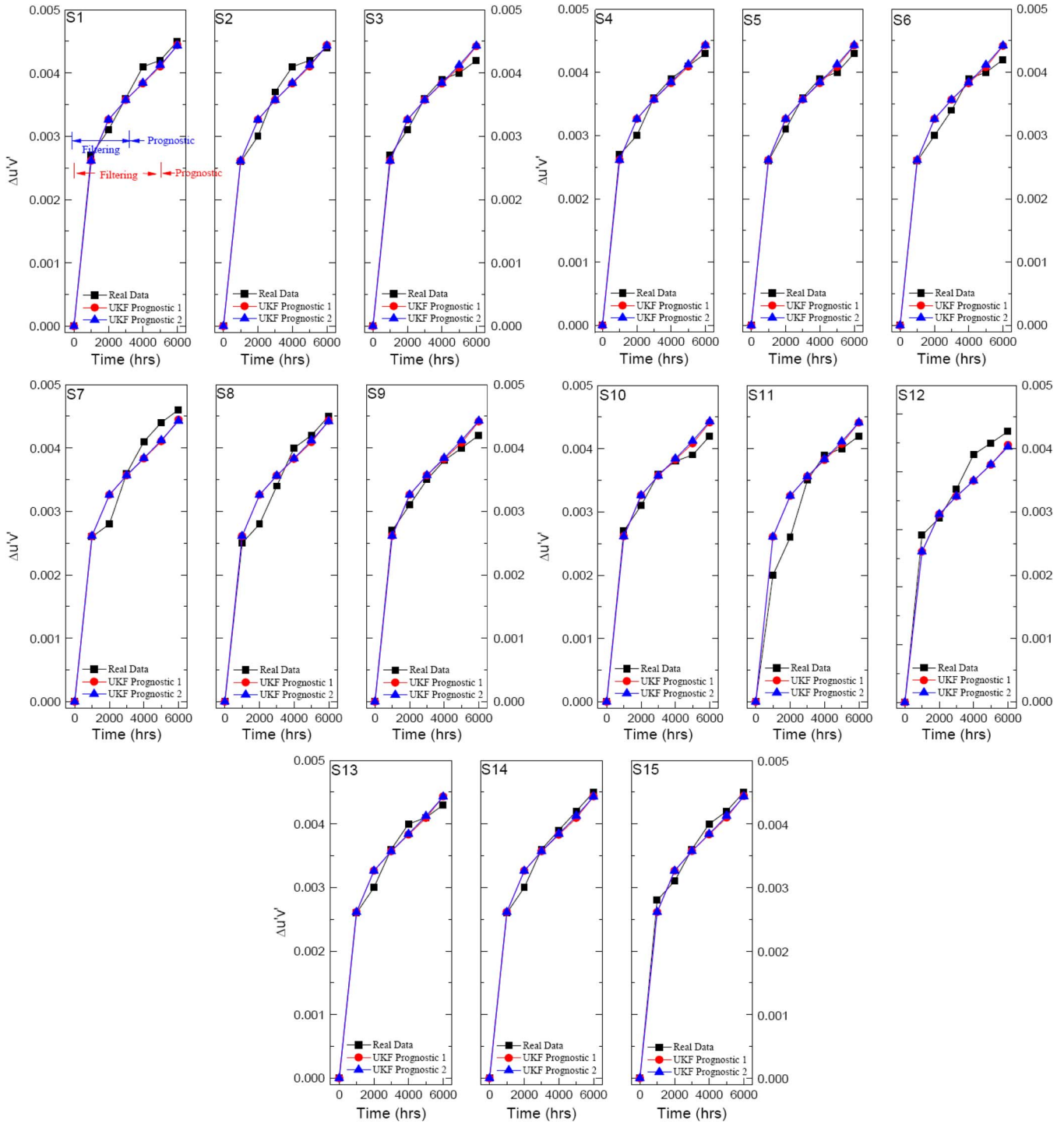


Fig. 13. Prognostic results of chromaticity state shift with UKF approach (Test samples S1-15).

of our proposed UKF approach. For example, the prognostics errors (Both UKF prognostic 1 starting from 5000 hrs and UKF prognostic 2 starting from 3000 hrs) can be controlled within 10% when we shortened the calibration test time from 6000 hrs to 5000 hrs. However, for the calibration test within 3000 hrs, the prognostics errors is large about 50%.

Thus, in our case, with implementing the UKF prognostic approach, the qualification testing plan can be improved as a combination testing with a 5000 hrs calibration test for ten training samples and a 3000 hrs test for fifteen test samples.

Compared to the recommended minimum testing time by IES LM-80-08 standard (6000 hrs), the UKF prognostic approach reduces the testing time to 5000 hrs and improves the efficiency of qualification testing.

V. CONCLUSION AND PROPOSALS

In the LED's reliability field, many previous studies have paid attention only to lumen depreciation failure in LED products, ignoring another common failure mode called

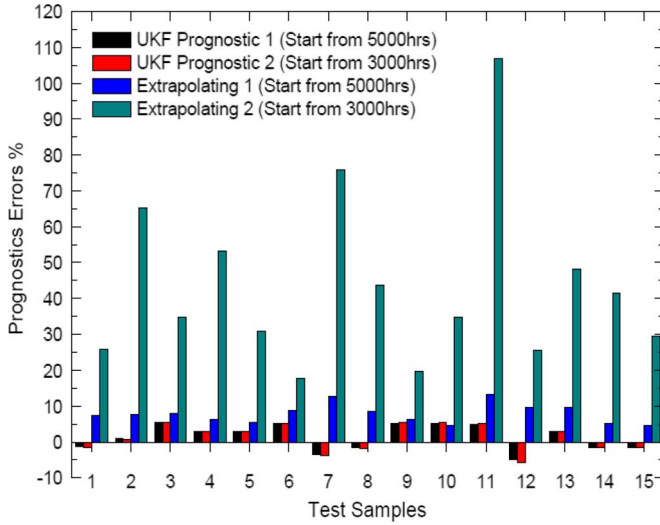


Fig. 14. Prognostics errors.

TABLE IV
PROGNOSTIC RMSE RESULTS

| State Prognostic Method | RMSE |
|-------------------------|--------|
| UKF Prognostic 1 | 3.70% |
| UKF Prognostic 2 | 3.90% |
| Extrapolating1 | 8.31% |
| Extrapolating2 | 49.32% |

TABLE V
INITIAL STATES ESTIMATED FROM DIFFERENT CALIBRATION TESTS

| Test time (hrs) | | a_0 | b_0 | c_0 | d_0 |
|-----------------|----------|-------------|-------------|-----------|----------|
| 3000 | Mean | 0.0021516 | 0.000184 | -0.00215 | -0.00525 |
| | Variance | 3.32998E-08 | 1.34E-09 | 3.37E-08 | 9.16E-07 |
| 4000 | Mean | 0.0024781 | 0.00012 | -0.00248 | -0.00306 |
| | Variance | 1.06874E-08 | 2.18E-10 | 1.09E-08 | 2.29E-07 |
| 5000 | Mean | 0.0027792 | 8.31E-05 | -0.00275 | -0.00201 |
| | Variance | 1.86944E-08 | 1.18E-10 | 1.03E-08 | 4E-07 |
| 6000 | Mean | 0.0029479 | 0.000065625 | -0.002933 | -0.0017 |
| | Variance | 2.3989E-08 | 1.71632E-10 | 2.063E-08 | 9.35E-08 |

chromaticity shift. In this paper, the chromaticity state was considered as a health indicator of pc-white LEDs in addition to lumen maintenance.

To accelerate the qualification testing for pc-white LEDs before being released to market, this paper used a prognostic approach to predict the future chromaticity state of pc-white LEDs based on the short-term collected data. The Euclidean distance between the original chromaticity coordinate and future coordinates in the CIE1976 color space (u' , v') was used to represent the chromaticity state shift and modeled as a nonlinear dual-exponential model. A recursive UKF prognostic approach was used to predict the chromaticity state of the pc-white LED. With the UKF approach, the prognostic root mean square error is lower than the error found in the extrapolated results, because UKF takes all of the information from the collected data at each test cycles into consideration and updates the state model from new measurement inputs step by step.

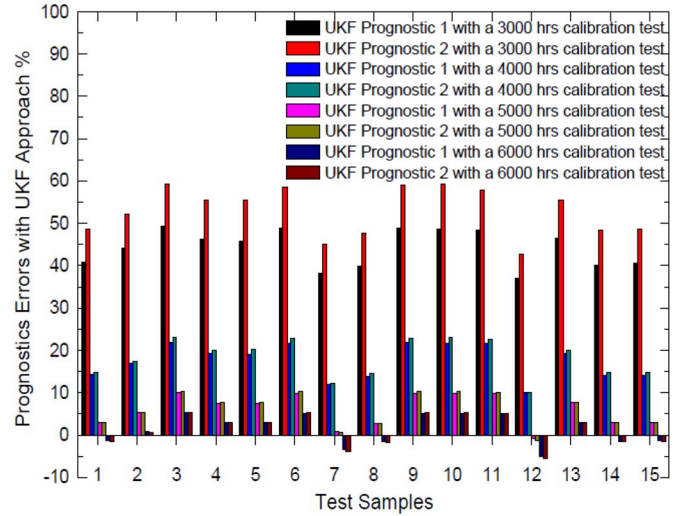


Fig. 15. Prognostics errors of UKF approaches with different calibration tests.

Additionally, this paper also conducted a sensitivity analysis of the prognostic performance of the proposed UKF approach by changing in the values of the initial states which were estimated from different calibration tests. The result shows the values of initial states can influence the prognostic performance of our method. Thus, with considering this finding, the qualification testing plan can be improved as a combination test with a 5000 hrs calibration test for ten training samples and a 3000 hrs test for fifteen test samples. Compared to the recommended minimum testing time by IES LM-80-08 standard (6000 hrs), the UKF prognostic approach reduces the testing time to 5000 hrs and improves the efficiency of qualification testing.

REFERENCES

- [1] E. F. Schubert and J. K. Kim, "Solid-state light sources getting smart," *Science*, vol. 308, no. 5726, pp. 1274–1278, May 27, 2005.
- [2] E. F. Schubert, *Light-Emitting Diodes*, 2nd ed. Cambridge: Cambridge University Press, 2006.
- [3] P. Mottier, *LEDs for Lighting Applications*. Hoboken, NJ, USA: Wiley, 2009.
- [4] R. Lenk and C. Lenk, *Practical Lighting Design With LEDs*. Hoboken, NJ, USA: Wiley, 2011.
- [5] W. Nelson, *Accelerated Testing: Statistical Methods, Test Plans, and Data Analysis*. New York, NY, USA: Wiley, 1990.
- [6] J. J. Fan, K.-C. Yung, and M. Pecht, "Lifetime estimation of high-power white LED using degradation-data-driven method," *IEEE Trans. Dev. Mater. Reliab.*, vol. 12, no. 2, pp. 470–477, Jun. 2012.
- [7] J. J. Fan, K. C. Yung, and M. Pecht, "Physics-of-failure-based prognostics and health management for high-power white light-emitting diode lighting," *IEEE Trans. Dev. Mater. Reliab.*, vol. 11, no. 3, pp. 407–416, Sep. 2011.
- [8] S. T. Tsaing and C.-Y. Peng, "Stochastic diffusion modeling of degradation data," *J. Data Sci.*, vol. 5, no. 3, pp. 315–333, 2007.
- [9] H. Liao and E. A. Elsayed, "Reliability inference for field conditions from accelerated degradation testing," *Nav. Res. Logist.*, vol. 53, no. 6, pp. 576–587, Sep. 2006.
- [10] T. Sutharssan, S. Stoyanov, C. Baileyemail, and Y. Rosunally, "Prognostics and health monitoring of high power LED," *Micromachines*, vol. 3, no. 1, pp. 78–100, 2012.
- [11] *Electrical and Photometric Measurements of Solid-State Lighting Products*, IES-LM-79-08, 2008.
- [12] *Approved Method for Lumen Maintenance Testing of LED Light Source*, IES-LM-80-08, 2008.
- [13] Solid-State Lighting Product Quality Initiative, "LED luminaire lifetime recommendations for testing and reporting, 2nd edition," Next Gen. Light Ind. Alliance with the U.S. Dept. Energy, Washington, DC, USA, 2011.

- [14] *Specifications for the Chromaticity of Solid State Lighting Products: For Electric Lamps*, ANSI/ANSI C78.377-2011, 2011, National Electrical Manufacturers Association/American National Standard Lighting Group, Rosslyn, VA, USA.
- [15] M. A. Alam, M. H. Azarian, M. Osterman, and M. Pecht, "Prognostics of failures in embedded planar capacitors using model-based and data-driven approaches," *J. Intell. Mater. Syst. Struct.*, vol. 22, no. 12, pp. 1293–1304, Aug. 2011.
- [16] C. Sankavaram, B. Pattipati, A. Kodali, K. Pattipati, M. Azam, S. Kumar, and M. Pecht, "Model-based and data-driven prognosis of automotive and electronic systems," in *Proc. IEEE Int. Conf. Autom. Sci. Eng.*, 2009, pp. 96–101.
- [17] M. Pecht, *Prognostics and Health Management of Electronics*. Hoboken, NJ, USA: Wiley, 2008.
- [18] M. H. Chang, D. Das, P. V. Varde, and M. Pecht, "Light emitting diodes reliability review," *Microelectron. Reliab.*, vol. 52, no. 5, pp. 762–782, May 2012.
- [19] M. Meneghini, L.-R. Trevisanello, G. Meneghesso, and E. Zanoni, "A review on the reliability of GaN-based LEDs," *IEEE Trans. Dev. Mater. Reliab.*, vol. 8, no. 2, pp. 323–331, Jun. 2008.
- [20] H. Luo, K.-S. Kim, E. F. Schubert, J. Cho, C. Sone, and Y. Park, "Analysis of high-power packages for phosphor-based white-light-emitting diodes," *Appl. Phys. Lett.*, vol. 86, no. 24, pp. 243505-1–243505-3, Jun. 13, 2005.
- [21] Y. C. Hsu, Y.-K. Lin, M.-H. Chen, C.-C. Tsai, J.-H. Kuang, S.-B. Huang, H.-L. Hu, Y.-I. Su, and W.-H. Cheng, "Failure mechanisms associated with lens shape of high-power LED modules in aging test," *IEEE Trans. Electron Dev.*, vol. 55, no. 2, pp. 689–694, Feb. 2008.
- [22] "Luxeon," Philips, San Jose, CA, USA, Technical Datasheet DS56, 2008.
- [23] Z. Y. Liu, S. Liu, and K. Wang, "Status and prospects for phosphor-based white LED packaging," *Front. Optoelectron. China*, vol. 2, no. 2, pp. 119–140, Jun. 2009.
- [24] S. Ye, F. Xiao, Y. X. Pan, Y. Y. Ma, and Q. Y. Zhang, "Phosphors in phosphor-converted white light-emitting diodes: Recent advances in materials, techniques and properties," *Mater. Sci. Eng. R, Rep.*, vol. 71, no. 1, pp. 1–34, Dec. 2010.
- [25] "Luxeon," Philips, San Jose, CA, USA, DR04: LM-80 Test Report, 2011.
- [26] *The IESNA Light Handbook: Reference and Application*, 9th ed. New York, NY, USA: IESNA, 2000.
- [27] J. Schanda, *Colorimetry: Understanding the CIE System*. Hoboken, NJ, USA: Wiley, 2007.
- [28] N. Narendran, L. Deng, J. P. Freyssinier, H. Yu, Y. Gu, D. Cyr, and J. Taylor, "Developing color tolerance criteria for white LEDs," Lighting Res. Center, Troy, NY, USA, Jan. 26, 2004.
- [29] *ENERGY STAR Program Requirements for SSL Luminaires, Version 1.1*, DoE, Washington, DC, USA, Dec. 19, 2008.
- [30] S. J. Julier and J. K. Uhlmann, "Unscented filtering and nonlinear estimation," *Proc. IEEE*, vol. 92, no. 3, pp. 401–422, Mar. 2004.
- [31] S. J. Julier, J. K. Uhlmann, and H. F. Durrant-Whyte, "A new approach for filtering nonlinear systems," in *Proc. Amer. Control Conf.*, 1995, pp. 1628–1632.
- [32] E. A. Wan and R. van der Merwe, "The unscented Kalman filter for nonlinear estimation," in *Proc. IEEE Adaptive Syst. Signal Process., Commun., Control Symp.*, 2000, pp. 153–158.
- [33] D. Simon, *Optimal State Estimation: Kalman, H [Infinity] and Nonlinear Approaches*. Hoboken, NJ, USA: Wiley, 2006.
- [34] S. Jafarzadeh, C. Lascu, and M. S. Fadali, "State estimation of induction motor drives using the unscented Kalman filter," *IEEE Trans. Ind. Electron.*, vol. 59, no. 11, pp. 4207–4216, Nov. 2012.
- [35] *ASSIST Recommendation: LED Life for General Lighting*, Lighting Res. Center, Troy, NY, USA, 2005.
- [36] *Projecting Long Term Lumen Maintenance of LED Light Sources*, IES-TM-21-11, 2011.
- [37] B. Gibbs, *Advanced Kalman Filtering, Least-Squares and Modeling*. Hoboken, NJ, USA: Wiley, 2011.

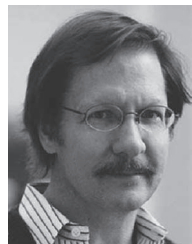


Jiajie Fan (S'12) received the B.S. degree in inorganic materials science and engineering from Nanjing University of Technology, Nanjing, China, in 2006 and the M.S. degree in material science and engineering from East China University of Science and Technology, Shanghai, China, in 2009. He is currently working toward the Ph.D. degree in industrial and systems engineering at The Hong Kong Polytechnic University, Kowloon, Hong Kong. His research interests include prognostics and health management for LED lighting and electronic assembly. He is a member of the IEEE Industrial Electronics and Components, Packaging, and Manufacturing Technology Societies. He is also a Student Member of the American Society for Quality and a Registered Member of certified Six Sigma Green Belt in Hong Kong Society for Quality.



Kam-Chuen Yung (M'12) received the B.Eng. degree from The University of Sydney, Sydney, Australia; the M.Sc. (Eng.) degree from The University of Hong Kong, Pokfulam, Hong Kong; and the Ph.D. degree from Brunel University, Uxbridge, U.K.

He is currently an Associate Professor with the Department of Industrial and Systems Engineering (ISE), The Hong Kong Polytechnic University (PolyU), Kowloon, Hong Kong. He has 28 years of experience in both academia and industry with engineering and management responsibilities. He is the Founder and Center-in-Charge of the Printed Circuit Board Technology Centre, ISE, PolyU. His research areas include printed-circuit-board technology, integrated-circuit manufacture, electronic assemblies and packaging, electronic materials, quality engineering, ISO9000 quality systems, TQM, and technology management.



Michael Pecht (F'92) received the M.S. degree in electrical engineering and the M.S. and Ph.D. degrees in engineering mechanics from the University of Wisconsin-Madison, Madison, WI, USA.

He is the Founder of the Center for Advanced Life Cycle Engineering, University of Maryland, College Park, MD, USA, where he is also a George Dieter Chair Professor in mechanical engineering and a Professor in applied mathematics. He has written more than 20 books on electronic-product development and use and supply-chain management and more than 400 technical articles. He has been leading a research team in the area of prognostics for the past 10 years and has now formed a new Prognostics and Health Management Consortium at the University of Maryland. He has consulted for more than 100 major international electronics companies, providing expertise in strategic planning, design, test, prognostics, IP, and risk assessment of electronic products and systems.

Dr. Pecht is a Professional Engineer and a Fellow of ASME and IMAPS. He served as the Chief Editor of the IEEE TRANSACTIONS ON RELIABILITY for eight years and on the Advisory Board of the IEEE SPECTRUM. He is also the Chief Editor of *Microelectronics Reliability*. He is an Associate Editor of the IEEE TRANSACTIONS ON COMPONENTS AND PACKAGING TECHNOLOGY. He was the recipient of the highest reliability honor, the IEEE Reliability Society's Lifetime Achievement Award, in 2008. He was also the recipient of the European Micro and Nano-Reliability Award for outstanding contributions to reliability research, the 3M Research Award for electronics packaging, and the IMAPS William D. Ashman Memorial Achievement Award for his contributions in electronics reliability analysis.